Carrier-envelope phase-dependent electronic conductivity in an air filament driven by few-cycle laser pulses

Lifeng Wang,[1,2] Xin Lu,[1] Hao Teng,[1,*] Tingting Xi,[3] Shiyou Chen,[1] Peng He,[1,4] Xinkui He,[1] and Zhiyi Wei[1,†]

[1]*Beijing National Laboratory for Condensed Matter Physics, Institute of Physics, Chinese Academy of Sciences, Beijing 100190, China*

[2]*Department of Laser Medicine, General Hospital of PLA, Beijing 100853, China*

[3]*School of Physics, University of Chinese Academy of Sciences, Beijing 101407, China*

[4]*School of Physics and Opto-Electronic Engineering, Xidian University, Xian 710071, China*

(Received 28 July 2014; published 13 July 2016)

The modulation of the electron conductivity in an air filament, which is produced by carrier-envelope phase (CEP) stabilized 7-fs laser pulses, is realized experimentally. Numerical results based on a coupled 3D+1 generalized nonlinear Schrödinger equation including the real electric-field dependent ionization model are in good agreement with those from the experiment. It is demonstrated that the CEP effect on the electron density originates from the CEP-induced modification of the electric field of the laser pulse, and this modification is amplified during nonlinear propagation. The results provide important information to help understand the physical mechanism of the filaments driven by few-cycle femtosecond laser pulses.

DOI: 10.1103/PhysRevA.94.013827

The interaction of laser and plasma has been investigated intensively for several decades. Driving laser pulses with durations of tens to hundreds of femtoseconds have been used in previous studies, such as generation of high-energy electron beams, laser lightening, coherent THz emission, keV x-ray radiation, and biological imaging [1–5]. In recent years, thanks to the state-of-art technologies of intense few-cycle lasers [6,7], the interaction of carrier-envelope phase (CEP) stabilized few-cycle laser pulses with different targets is investigated under extreme conditions to trigger and resolve new physical processes at unprecedented time resolution. When sub-10-fs laser pulses were focused into solid targets, strong overdense plasma with high temperature was generated [8], a pronounced increase of the absorption of p polarization at increasing angles was recorded to be 77% [9], and direct acceleration of electrons to 150 keV with very narrow angular distribution was observed [10]. The accelerated electron pulses and plasma waves in helium were obtained in real time [11].

The interaction of the few-cycle lasers with air plasma opens the way to explore the new phenomena originated from electrons in the air filament. If the electronic processes are resolved, the evolution of the filament will be well understood. For example, the CEP dependence of THz radiation for 8-fs laser pulses at 800 nm has been reported by Kreß *et al.* They clarified the THz emission was sensitive to the electric field which was modulated by the initial CEP. But the propagation effect of the 8-fs laser beam in air was ignored in their interpretation [12]. However Bergé *et al.* theoretically demonstrated that the electric field was distorted during the propagation process in air. Furthermore, the additional phase shift was induced by third-harmonic generation and plasma effect, while the filament could also be affected by the CEP when the pulse duration closed to the few-cycle regime. These interpretations have not been verified experimentally [13]. In 2010, Laban *et al.* predicted that the length of the filament generated by 6.3-fs laser pulses in air should change by 790-μm the CEP shifted $\pi/2$ rad; to the best of our knowledge, there is no clear experimental evidence to support this prediction [14]. In fact, the CEP effect during the interaction between the laser and air filament has not been fully investigated.

In this paper, the experimental measurement of the electron conductivity of the filament generated by 7-fs laser pulses in air was reported. The advantages of using the few-cycle laser pulses are (1) only one filament is formed and (2) the CEP effect can be controlled precisely in the experiment. Clear evidence of the CEP effect on the electron conductivity in the filament was observed, which shows strong modulation of electron density with the CEP, and the maximum modulation depth was 23.7%. By numerically solving a coupled 3D+1 generalized nonlinear Schrödinger equation, it was demonstrated that the effect of the initial CEP in the air filament was preserved and enhanced by the optical nonlinearity during the propagation of laser pulses in air.

The laser system is shown in Fig. 1(a). A commercial Ti:sapphire chirped-pulse amplifier (Femtolaser Compact PRO) delivers 25-fs, 0.8-mJ laser pulses at 1-kHz repetition rate. The laser pulses are further spectrally broadened in a differentially pumped neon-filled hollow fiber and temporally compressed by the chirped mirrors [15]. The CEPs of the laser pulses are actively stabilized with fluctuation of 85 mrad in more than 7 h by locking both the oscillator and amplifier loops. Finally, compression of 0.25-mJ laser pulses to below 7 fs is obtained [16]. As shown in Fig. 1(b), the intense 7-fs laser pulses were focused in air with a 500-mm focal length concave silver mirror, and two thin copper plates were located between the focal point as electrodes. A laser beam was used to drill holes in the copper plates, which let the laser pulses go through, and a filament was generated. According to the fluorescence of the filament, the distance between two copper electrodes is chosen to be 10 mm in the center of the filament in order to improve the signal-to-noise ratio. The discharging circuit system, which was used to measure the conductivity of the filament, was formed by the filament, two copper plates, a high-voltage supply (200 V), and an oscilloscope. The typical voltage signal detected by the oscilloscope is the decay signal, as shown in Fig. 1(c).

*hteng@iphy.ac.cn
†zywei@iphy.ac.cn

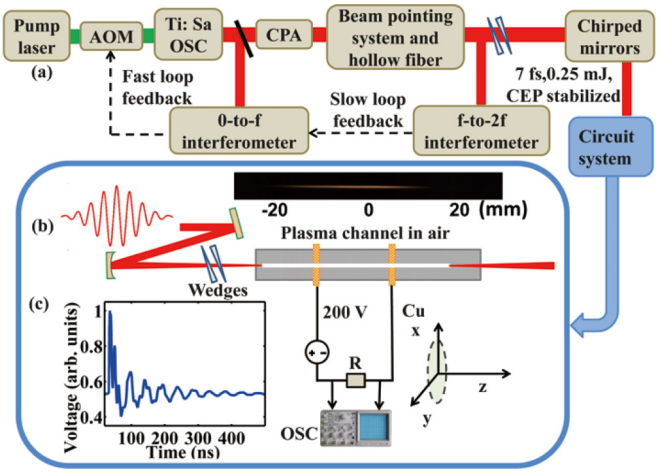

FIG. 1. Schematic of the experiment. (a) The laser system includes an acousto-optical modulator (AOM) and chirped pulse amplification (CPA). The 0-to-f and f-to-2f interferometers are controlled by the fast and slow feedback loops through the AOM, respectively. (b) Schematic of the circuit system used to measure the electron conductivity in the laser induced filament. (c) The voltage signal detected by an oscilloscope.

Figure 2 shows the maximum voltage of the discharging signal as a function of the CEP of the driving laser pulses. The step of the CEP was $\pi/20$, and the voltage signal was recorded by integrating over 10 000 pulses (it took 0.5 h to measure the voltage over a range of 2π). When the CEP was locked, a clear modulation with the CEP appeared, as shown in Fig. 2(a). The period of the voltage modulation was π. The modulation depth was 23.7%. However, when the CEP was not locked, the voltage stayed as a constant, which meant the strong modulation did come from the CEP of the driving laser pulses.

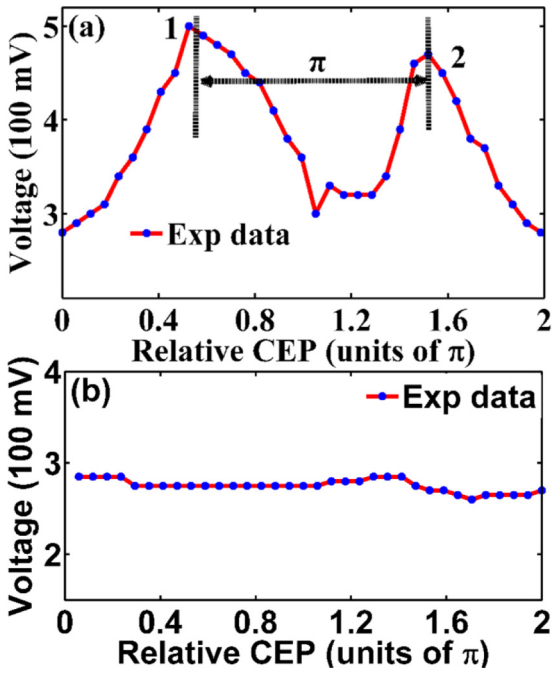

FIG. 2. Comparison of the maximum voltage signal with locked (a) and unlocked (b) CEP.

The free electrons in the filament are mainly contributed by the ionization in oxygen because of its lower ionization potential (compared to nitrogen) in the propagation of laser pulses in air. According to the collision theory [17], the filament is conductive and the maximum voltage signal is proportional to the conductivity of the filament. In order to explain the experimental results, we modeled the propagation of a few-cycle laser pulse in air by the coupled 3D+1 generalized nonlinear Schrödinger equation for the pulse envelope [18–21], which is expressed as

$$\frac{\partial A}{\partial z} = \frac{i}{2k_0}T^{-1}\triangle_\perp A + iD(i\partial_\tau)A + ik_0n_2T|A|^2A - i\frac{k_0}{2}T^{-1}\frac{\omega_{pe}^2(\rho)}{\omega_0^2}A - \frac{1}{2}\frac{\partial\rho}{\partial t}\frac{I_p}{|A|^2}A, \quad (1)$$

where A is the laser electric-field envelope, z is the propagation distance, and k_0 and ω_0 are the central wave number and frequency. The Laplacian operator $\triangle_\perp$ denotes the beam transverse diffraction. $T = (1 + \frac{i}{\omega_0}\partial_t)$, $T^{-1}\triangle_\perp A$ accounts for the space-time focusing, and $T|A|^2A$ accounts for the self-steepening of the pulse. $D = \sum_{n=2}^{+\infty}(\partial^n k/\partial\omega^n|_{\omega=\omega_0}/n!)(i\partial_t)^n$ describes to the dispersion of the air [22]. The nonlinear index of the refraction $n_2 = 3.2 \times 10^{-19}$ cm^2/W describes the self-focusing effect due to the Kerr response of the air. The plasma frequency is $\omega_{pe} = [e^2\rho/(m_e\epsilon_0)]^{1/2}$ with e, m_e, ρ, and ϵ_0 being the electron charge, mass, density, and vacuum permittivity. The absorption of the plasma is described by the last term, where $I_p = 12.1$ eV is the ionization potential of oxygen. In order to describe the CEP effect on the electron density of the filament, the ADK (Ammosov, Delone, and Krainov) model was employed in this work [23] to describe the instantaneous electric-filed dependent ionization. The electron density is expressed as

$$\frac{\partial\rho(t)}{\partial t} = (\rho_0 - \rho)w(t), \quad (2)$$

$$\rho(t) = \rho_0\left\{1 - \exp\left[-\int_{-\infty}^{t} w(t')dt'\right]\right\}, \quad (3)$$

$$w(t) = \omega_p|C_{n^*}|^2\left(\frac{4\omega_p}{\omega_t}\right)^{2n^*-1}\exp\left(-\frac{4\omega_p}{3\omega_t}\right), \quad (4)$$

where $\omega_p = I_p/\hbar$ and $\omega_t = e|E(t)|^2/\sqrt{2m_eI_p}$, $n^* = Z(I_{ph}/I_p)^{1/2}$, $|C_{n^*}|^2 = 2^{2n^*}/[n^*\Gamma(n^*+1)\Gamma(n^*)]$. I_{ph} is the ionization potential of hydrogen. $E(t)$ is the instantaneous electric field of the laser, which can be calculated from the complex amplitude as $E(t) = \mathrm{Re}\{A(t)\exp(i\omega_0 t)\}$. $\hbar$ is Planck's constant, and Z is the resulting net charge of the atom. $\rho_0 = 5.4 \times 10^{18}$ cm^{-3}. In our simulation, a 7-fs Gaussian laser pulse is used, with the envelope of the laser pulse given by $A(x,y,z,t)|_{z=0} = A_0\exp[-(x^2+y^2)/r_0^2 - t^2/\tau^2]\exp(i\varphi_{\mathrm{CE}})$, where the pulse duration $\Delta T = \sqrt{2ln2}\tau_0 = 7$ fs. By numerical solving Eqs. (1)–(4) with the full step fast Fourier transform method in space and time with a 19.9-μm spatial and 0.07-fs temporal resolution, we obtain the spatial-temporal distribution of the electron density in the filament along the propagation direction.

Figure 3(a) gives the simulated spatial distribution of electron density in the filament produced by a 7-fs laser pulse

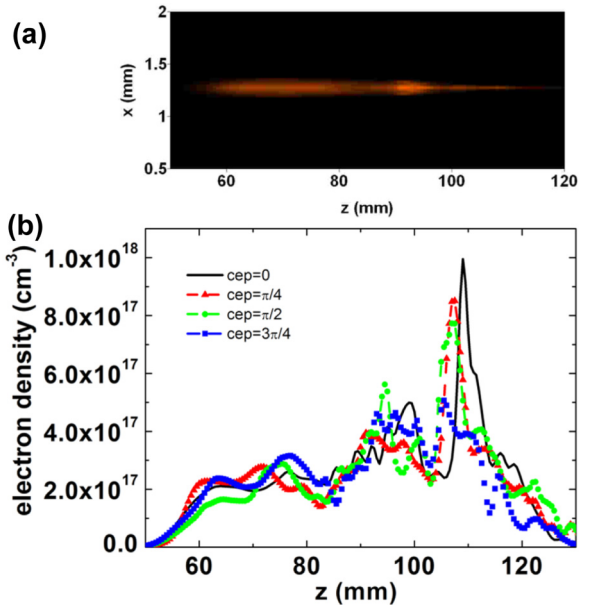

FIG. 3. (a) Spatial distribution of the electron density in the filament from the solution of the nonlinear Schrödinger equation. (b) Distribution of on-axis electron density in the range $50 < z[\text{mm}] < 130$ for different CEP.

with averaged CEP. In order to see the details, the spatial distribution of on-axis electron density is shown in Fig. 3(b) for four φ_{CE} values, where obvious differences could be observed. For the $\varphi_{\text{CE}} = 0$ (black solid line), there are two peaks along the propagation axis. The intensity of the higher one ($z = 110$ mm) is two times that of the lower one ($z = 99$ mm). As the CEP shifted to $\pi/2$ (green dashed line with circle), there are two relatively weak peaks. When $\varphi_{\text{CE}} = 3\pi/4$ (blue dashed line with rectangle), there is no obvious peak. It is shown that the maximum position of the on-axis electron density is shifted by the initial CEP. The electron density distribution is sensitive to the initial CEP.

In order to explore the dynamics of the 7-fs laser pulses during the propagation, the electric fields are plotted as a function of propagation distances and initial CEPs, which are shown in Fig. 4. In the simulation results [in Fig. 4(a) where $\varphi_{\text{CE}} = 0$], four values of z were selected between 0 and 200 mm. In the early stage of propagation, the electric field maintains a good Gaussian shape in time (at$z = 50$ mm). During the interaction with air, the laser field is strongly distorted by the nonlinear propagation effect, especially near the focus. The leading part of the pulse is redshifted and the trailing part is blueshifted, and it is difficult to define the CEP at this range (for example, $z = 70$ mm). In order to clarify the CEP effect, the on-axis electric fields with different CEPs at $z = 109$ mm are shown in Fig. 4(b). It is clear that the electric-field structure is sensitive to the initial CEP. The differences of the electric filed, which are induced by the initial CEP during the propagation of few-cycle laser pulses in air, lead to the difference of the spatial and temporal distributions of the electron density. Furthermore, the electron conductivity of the filament is affected by the CEP.

For a 7-fs Gaussian pulse, the maximum electric-field difference is only 1.5% for $\varphi_{\text{CE}} = 0$ and $\pi/2$; how can we

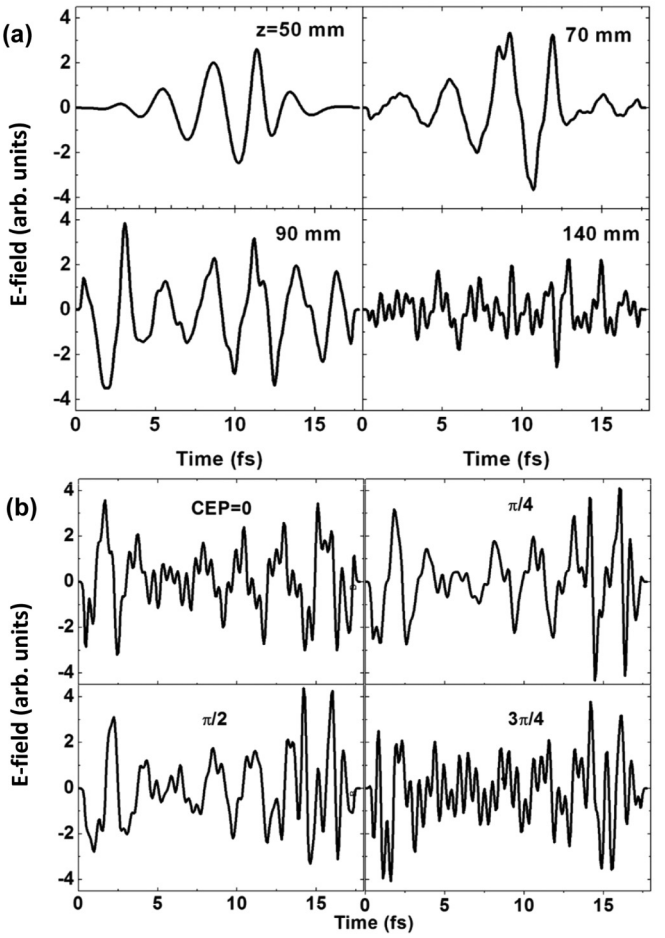

FIG. 4. (a) On-axis electric field at different z for $\varphi_{\text{CE}} = 0$ and (b) on-axis electric field at $z = 109$ mm for four φ_{CE}.

observe a modulation depth of 23.7%? In order to compare with the experimental observations, electron conductivity was calculated under two different conditions. After integration over space and time (with a spatial and temporal range of

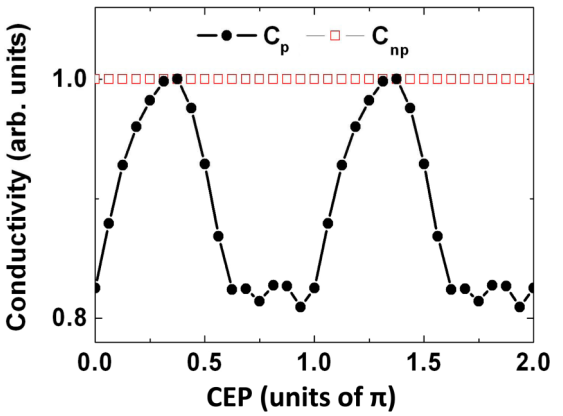

FIG. 5. Comparison of the conductivities as a function of CEP under two conditions. After making the integration over space and time, the red curve with hollow rectangles (C_{np}) and the black curve with solid circles (C_p) are the calculated conductivity without and with propagation effects, respectively.

3.36 mm and 23.6 fs), clear differences of the electron conductivity with and without nonlinear propagation effect were shown in Fig. 5. The red curve with hollow rectangles (C_{np}) is the conductivity calculated by applying the same parameters mentioned above but without nonlinear propagation effect, and there is not any modulation induced by the CEP, while the black curve with solid circles (C_p) is the conductivity calculated with nonlinear propagation effect. The modulation depth is 11.1%, which is comparable with the experimental measurement. Although the difference of the electric field induced by the initial CEP is less than 2%, it is increased by ten times as the pulse propagates.

In conclusion, the electron conductivity of an air filament driven by CEP stabilized 7-fs laser pulses was measured. The strong modulation of the electron conductivity, the modulation depth of which is 23.7%, was observed to be dependent on the CEP with a period of π. The results are consistent with those of a model calculation based on a generalized Schrödinger equation including electric-field dependent ionization. The simulation results show that the phase shift is sensitive to the initial conditions and the difference induced by the initial CEP is preserved during the propagation of few-cycle laser pulses. The modulation of electron density originates from the modification of the laser electric field, which is amplified by nonlinear propagation effect.

We acknowledge fruitful discussion with Mingyang Yu, Peng Ye, and Shiyang Zhong and important advice from Dehua Li and Wenjun Liu. This work is partly supported by the National Key Technology Research and Development Program of the Ministry of Science and Technology (Grant No. 2012BAC23B03), National Basic Research Program of China (Grant No. 2013CBA01501), National Key Basic Research Program of China (Grants No. 2013CB922401 and No. 2013CB922402), and National Natural Science Foundation of China (Grants No. 11074298 and No. 11574387).

[1] W. Leemans and E. Esarey, Phys. Today. **62**, 44 (2009).
[2] Jérôme Kasparian and Jean-Pierre Wolf, Opt. Express. **16**, 466 (2008).
[3] J. van Tilborg, C. B. Schroeder, C. V. Filip, Cs. Tóth, C. G. R. Geddes, G. Fubiani, R. Huber, R. A. Kaindl, E. Esarey, and W. P. Leemans, Phys. Rev. Lett. **96**, 014801 (2006).
[4] S. Kneip, C. McGuffey, J. Martins, S. Martins, C. Bellei, V. Chvykov *et al.*, Nat. Phys. **6**, 980 (2010).
[5] S. Kneip, C. McGuffey, F. Dollar, M. S. Bloom, V. Chvykov, G. Kalintchenko, K. Krushelnick, A. Maksimchuk, S. P. D. Mangles, T. Matsuoka, Z. Najmudin, C. A. J. Palmer, J. Schreiber, W. Schumaker, A. G. R. Thomas, and V. Yanovsky, Appl. Phys. Lett. **99**, 093701 (2011).
[6] T. Fuji, J. Rauschenberger, A. Apolonski, V. S. Yakovlev, G. Tempea, T. Udem, C. Gohle, T. W. Hänsch, W. Lehnert, M. Scherer, and F. Krausz, Opt. Lett. **30**, 332 (2005).
[7] H. R. Telle, G. Steinmeyer, A. E. Dunlop, J. Stenger, D. H. Sutter, and U. Keller, App. Phys. B. **69**, 327 (1999).
[8] J. Osterholz, F. Brandl, T. Fischer, D. Hemmers, M. Cerchez, G. Pretzler, O. Willi, and S. J. Rose, Phys. Rev. Lett. **96**, 085002 (2006).
[9] M. Cerchez, R. Jung, J. Osterholz, T. Toncian, O. Willi, P. Mulser, and H. Ruhl, Phys. Rev. Lett. **100**, 245001 (2008).
[10] F. Brandl, B. Hidding, J. Osterholz, D. Hemmers, A. Karmakar, A. Pukhov, and G. Pretzler, Phys. Rev. Lett. **102**, 195001 (2009).
[11] A. Buck, M. Nicolai, K. Schmid, C. Sears, A. Sävert, J. Mikhailova, F. Krausz, M. Kaluza, and L. Veisz, Nat. Physics **7**, 543 (2011).
[12] M. Kreß, T. Löffler, M. D. Thomson, R. Dörner, H. Gimpel, K. Zrost, T. Ergler, R. Moshammer, U. Morgner, J. Ullrich *et al.*, Nat. Phys. **2**, 327 (2006).
[13] L. Bergé, C.-L. Soulez, C. Köhler, and S. Skupin, Appl. Phys. B. **103**, 563 (2011).
[14] D. E. Laban, W. C. Wallace, R. D. Glover, R. T. Sang, and D. Kielpinski, Opt. Lett. **35**, 1653 (2010).
[15] J. S. Robinson, C. A. Haworth, H. Teng, R. A. Smith, J. P. Marangos, and J. W. G. Tisch, Appl. Phys. B. **85**, 525 (2006).
[16] W. Zhang, H. Teng, C. Yun, P. Ye, M. Zhan, S. Zhong, X. He, L. Wang, and Z. Wei, Chin. Phys. Lett. **31**, 084204 (2014).
[17] H. D. Ladouceur, A. P. Baronavski, D. Lohrmann, P. W. Grounds, and P. G. Girardi, Opt. Commun. **189**, 107 (2001).
[18] P. Panagiotopoulos, D. G. Papazoglou, A. Couairon, and S. Tzortzakis, Nat. Commun. **4**, 2622 (2013).
[19] L. Bergé, Opt. Express **16**, 21529 (2008).
[20] T.-T. Xi, X. Lu, and J. Zhang, Phys. Rev. Lett. **96**, 025003 (2006).
[21] C. Gong, J. Jiang, C. Li, L. Song, Z. Zeng, Y. Zheng, J. Miao, X. Ge, Y. Deng, R. Li *et al.*, Opt. Express. **21**, 24120 (2013).
[22] E. R. Peck and K. J. Reeder, J. Opt. Soc. Am. **62**, 958 (1972).
[23] E. Priori, G. Cerullo, M. Nisoli, S. Stagira, S. De Silvestri, P. Villoresi, L. Poletto, P. Ceccherini, C. Altucci, R. Bruzzese *et al.*, Phys. Rev. A. **61**, 063801 (2000).